Submonolayer regime of Co epitaxy on Pd(111): Morphology and electronic structure

M. Wasniowska,[1,*] W. Wulfhekel,[1,2] M. Przybylski,[1] and J. Kirschner[1]
[1]*Max-Planck-Institut für Mikrostrukturphysik Weinberg 2, D-06120 Halle, Germany*
[2]*Physikalisches Institut, Universität Karlsruhe, Wolfgang-Gaede Strasse 1, 76128 Karlsruhe, Germany*
(Received 28 June 2007; revised manuscript received 2 June 2008; published 2 July 2008)

We report on the early stage of Cobalt growth on Pd(111) studied with scanning tunneling microscopy. The electronic structure of the islands grown at 550 and 300 K was studied with scanning tunneling spectroscopy at low temperatures. Triangular monolayer-high islands grown at 550 K show fcc or hcp stacking. The position and the intensity of the surface-state peak depend on the stacking of these islands. On the hexagonal double-layer islands grown at 300 K, a dislocation pattern appears, which contains atoms in fcc and hcp, as well as a dislocation line and top positions. Fcc and hcp regions show similar features in dI/dU spectra; however, the surface-state peak positions are slightly shifted. For these islands, spin-polarized STS measurements reveal a spin contrast reflecting perpendicular magnetization.

DOI: 10.1103/PhysRevB.78.035405 PACS number(s): 68.37.−d, 68.55.−a, 61.72.Ff

I. INTRODUCTION

Heteroepitaxy is an important tool in materials physics. Due to the crystallographic structure of the substrate, the film material may be stabilized in unusual modifications such that the film-substrate system has novel chemical and physical properties compared to the bulk.[1] The phenomena observed in ultrathin heteroepitaxial films are linked to the reduced dimensionality and the unique properties of the surface and interface regions resulting in modifications of the electronic structure. For this reason, magnetic thin films or islands on nonmagnetic substrates are model systems for studying magnetism and electronic properties in reduced dimensions. Moreover, films deposited on fcc (111) surfaces often show a large variety of different self-organized structures represented by different shapes of islands. In growth experiments carried out on fcc (111) and hcp (0001) substrates, it has been shown that changes in island structures result from deposition at different substrate temperatures and with different deposition fluxes.[2] Often the shape of an island is determined by kinetic processes. Island shapes can be subdivided into two general classes: ramified islands with rough island edges and compact islands with relatively straight island edges. The formation of the ramified islands takes place at relatively low temperatures, when the edge diffusion is frozen as, for example, in the heteroepitaxial growth of Au/Ru(0001) (Ref. 3) and in the homoepitaxial growth of Pt/Pt(111).[2] The shape of a compact island is controlled by the ability of the captured adatoms to diffuse along the island edges and cross corners.[2] Besides the various shapes of islands, fcc and hcp stackings of islands are often observed on fcc (111) surfaces. Meinel *et al.*[4] first reported transmission electron microscopy studies which showed that silver islands on Ag(111) show hcp or fcc stacking. Busse *et al.*[5] observed a similar phenomenon for the system Ir/Ir(111). The nucleation of stacking faults was also observed for heteroepitaxed systems. A prominent example is Co on Cu(111).[6] For this system, the difference between the electronic structures of fcc and hcp stackings was shown by means of scanning tunneling spectroscopy (STS). It is manifested as a shift of the surface-state energy. Besides these properties, spin-polarized measurements showed an out-of-plane spin contrast for triangular islands.[7]

The work presented in this paper is a study of the structural and electronic properties of submonolayer Co films on Pd(111). For this system, the combination of the fcc (111) surface of palladium with 9.1% misfit between Co and Pd induces a variety of different shapes of Co islands and poses an intriguing issue about electronic structure. Additionally, in Co/Pd(111) the direction of the easy magnetization axis is out of plane for film thickness below 1 monolayer (ML). To gain reliable information, the samples were studied *in situ* with scanning tunneling microscopy (STM), scanning tunneling spectroscopy (STS), and spin-polarized scanning tunneling spectroscopy (SP-STS). We show that at and below room temperature, the Co films grow in a mixture of fcc and hcp. We also present a combined STM and STS study of fcc and hcp islands. Using STS, we observe that the energy of the surface state depends on the stacking for the dislocation pattern of double-layer islands. By means of spin-polarized STS, we show that the surface state at +0.2 eV is spin polarized.

II. EXPERIMENT

The experiments were carried out in an ultrahigh vacuum (UHV) chamber with a base pressure better than 1×10^{-10} mbar. The Pd(111) single crystal was cleaned *in situ* by sputtering at 300 K with 1.5 keV Ar^+ ions followed by annealing at 870 K for 10 min. The sample temperature was measured with a thermocouple attached to the sample holder in close vicinity of the sample. Since the thermocouple was not directly contacted to the sample, the temperature of the crystal was calibrated with an infrared pyrometer. The temperature of the sample was varied between 180 K (cooling with liquid nitrogen) and 850 K (radiative heating). The cleanliness and the surface quality of the Pd crystal were checked by means of Auger electron spectroscopy (AES), low-energy electron diffraction (LEED), and STM. AES spectra of the single crystal showed no contamination within the detection limit of our spectrometer. Sharp (1×1) LEED patterns with threefold symmetry which are characteristic of

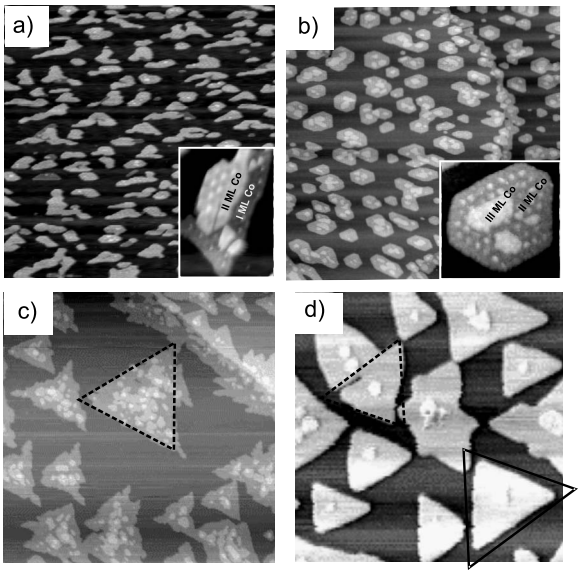

FIG. 1. Series of STM images of Co/Pd(111) showing the shape of the cobalt islands. In addition, this figure presents how the increase in adatom mobility results in lowering of the island density. The deposition temperatures are (a) 210 K (the 42×51 nm^2 inset shows both the 1- and 2-ML-high islands), (b) 300 K (the 47×40 nm^2 inset shows the DL island), (c) 495 K, and (d) 550 K. The deposited amounts are 0.6 ML in (a)–(d). The size of shown region is always 500×500 nm^2, and the deposition rate is $R=0.4$ ML/min. The single line (dashed line) triangle marks fcc (hcp) island.

clean fcc Pd(111) surface were observed. The STM measurements show average terrace sizes of a few hundred nanometers. Co (99.999% purity) was deposited on the Pd(111) by molecular beam epitaxy and the deposition rate was 0.4 ML/min (in substrate atomic density units). After the deposition, the sample was immediately transferred to the STM chamber to minimize further contamination and to avoid surface diffusion of Co atoms. The growth of Co on Pd(111) at submonolayer coverage has been studied with low-temperature STM *in situ*. During STS measurements, the sample was cooled to 77 K (homebuilt STM) or 30 K (variable temperature STM by Omicron). The differential conductivity dI/dU was obtained with tunneling spectroscopy using a lock-in technique. Typical tunneling parameters were $I=1-3$ nA, $U=\pm1$ V, and modulation of 30 mV at 30 K and 50 mV at 77 K.

III. MORPHOLOGY OF COBALT ISLANDS ON PALLADIUM(111)

Since the island growth has a large influence on the growth mode of thin films [two-dimensional (2D) or three-dimensional (3D) growth], first we briefly discuss the growth morphology of the islands at different deposition temperatures. Figure 1 shows STM images revealing a transition in island shape from ramified at low temperature to compact triangular islands at higher temperature through a compact hexagonal form at room temperature as discussed in detail in Ref. 8.

At 210 K, the islands have a ramified shape due to a limited diffusion along the step edges and around corners.[2] Furthermore, the height of the Co islands grown at 210 K varies. The islands can contain both 1- and 2-ML-high areas, the latter with weak dislocation network visible [see the inset of Fig. 1(a)].

At room temperature, Co grows by pure double-layer formation of hexagonal islands [see Fig. 1(b)]. The islands show a dislocation network as periodic white dots [see inset of Fig. 1(b)]. This suggests that the hexagonal shape is related to the dislocation network, i.e., the strain relaxation of Co on Pd.[8]

In the temperature range between 495 and 550 K, triangular single-layer islands form. The rim of the Co islands prepared at 495 K shows some dendrite tendencies. This behavior can be interpreted as intermixing between Co atoms and Pd at the edges of islands or could be related to strain relaxation at step edges.[9]

The STM observations show that there is already a three-dimensional growth of Co on Pd(111) in the submonolayer regime. At all temperatures, the second or third monolayer is formed on top of the islands before they coalesce. The three-dimensional growth mode of islands is due to a Schwoebel barrier which prevents higher-layer atoms from surmounting the edges of individual islands[10] and/or due to the large lattice mismatch between Co layer and the substrate; i.e., the next-layer island nucleation is induced by strain.[11]

For the next step, we focus on the electronic structure of Co islands grown on Pd(111) at different temperatures. We have chosen preparation temperatures of 300 and 550 K to compare the electronic structures of islands with different heights (single and double layer) as well as islands with and without dislocation network.

IV. STACKING FAULTS OF COBALT ISLANDS ON PALLADIUM(111)

In this section, the formation of stacking-faulted islands in the system Co/Pd(111) at 550 K is studied by means of scanning tunneling microscopy and spectroscopy.

A. Electronic structure of fcc and hcp islands as seen with STM

Before we discuss the electronic structure of fcc and hcp islands grown at 550 K as observed with STS, we focus on topographic STM images of fcc and hcp islands. STM does not directly image the topography of the surface; instead it images the electronic density of states. For this reason, a difference in stacking results in different apparent heights of fcc and hcp islands. Triangular islands with opposite orientations are visible in Fig. 2(a). The two island orientations can been explained by initial nucleation on the two different threefold hollow sites of the Pd(111) surface, thus leading to a stacking fault at the interface for one island orientation, whereas the other follows the fcc stacking of the substrate.

A careful inspection of the scan reveals that the hcp island appears lower than the fcc island. For the tunneling conditions applied in this image ($U=+0.2$ V and $I=2$ nA), the

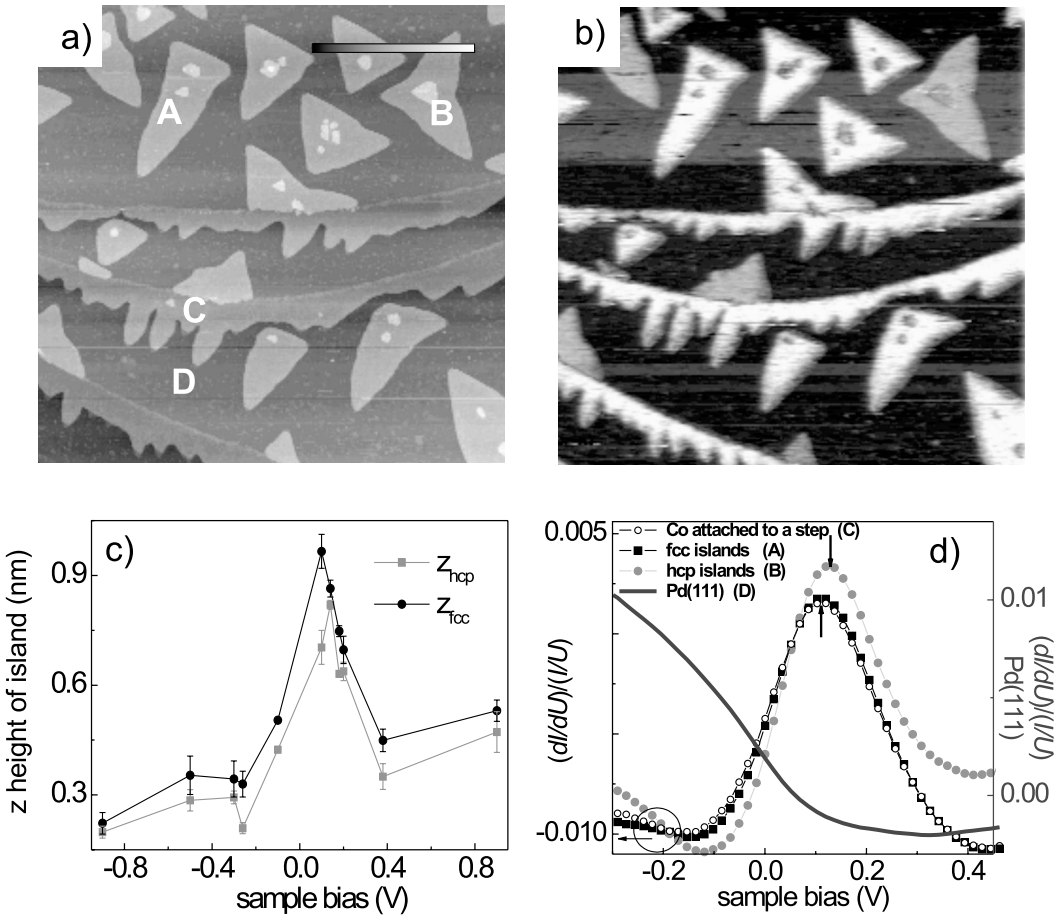

FIG. 2. (a) Constant current image and (b) dI/dU map of 1-ML-high Co islands on Pd(111) at $U=+0.15$ V. The scan area is 900 $\times 900$ nm^2. (c) Dependence of the heights of fcc and hcp islands on bias voltage for line scan along the line in (a). Results were obtained by voltage dependent constant current STM imaging with $I=2$ nA. (d) Tunneling spectra obtained at a set point of $U=1$ V and $I=1$ nA. The curves were averaged on two different types of islands and on Co atoms attached to a Pd step. The spectra of the two island types differ in peak position. The spectra for type-A islands and for Co atoms attached to the Pd step are almost identical, indicating that type-A islands are fcc islands.

height difference corresponds to $\Delta z=0.08\pm0.01$ nm. The electronic nature of this effect becomes apparent upon analyzing the line profile in Fig. 2(a) obtained with different bias voltages [see Fig. 2(c)]. Clearly, the fcc phase is imaged higher than the hcp phase for U between -1 and $+1$ V and this difference in apparent heights varies with bias voltage.

This is caused by different electronic structures of the fcc and hcp layers on a regular fcc substrate. In order to relate the voltage dependence of the STM images to the structural identity of Co islands, we performed STS at 30 K. The STS measurements allow identification of the respective stackings as depicted in Fig. 2(d).

B. STS of triangular Co islands

Simultaneous with topography, we measured $I(U)$ curves and the differential conductance dI/dU at every pixel of the image with stabilization parameters $I=2$ nA and $U=1$ V. Results are shown in Figs. 2(b) and 2(d). Images in Figs. 2(a) and 2(b) present the topography and the dI/dU map, respectively. The dI/dU curves are shown in Fig. 2(d), averaged over areas indicated by A, B, C, and D in Fig. 2(a).

Curve A is representative of fcc islands, while B belongs to faulted islands. A spectrum of Pd (D) is included for comparison with Co spectra. In the Co spectra the main feature is a strong peak slightly above the Fermi level. While the general curve shapes for the two types of islands are quite similar, the spectra differ by a slight shift in energy ($\Delta E \approx 30$ meV) of the peaks and higher intensity of the peak for hcp stacking spectrum.

The electronic difference becomes even more obvious when inspecting the dI/dU map. The fcc islands exhibit a higher local density of state (LDOS) (corresponding to the bright area) than faulted ones. In this dI/dU map we observe that islands attached to the step edge appear always bright. The Co atoms of these islands were captured at step edges, which implies a correct stacking since at a step edge, the perfect substrate stacking at the step edge is continued. We can compare the spectra of both types of islands and islands attached to the steps. The result is displayed in Fig. 2(d) (cf. curves A and C). Islands with corners in the same direction such as the attached islands have all identical spectra and are therefore fcc islands, while the islands of opposite orientation differ electronically from the island at step edges and are

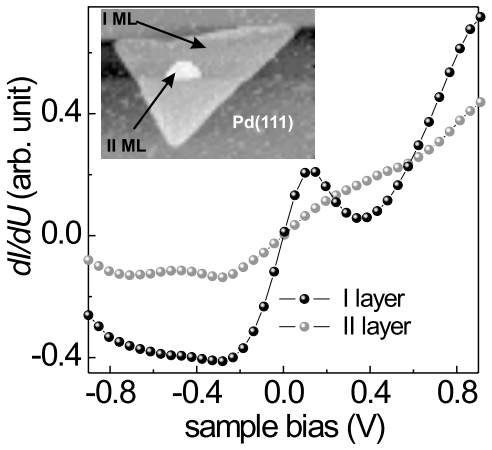

FIG. 3. The dI/dU curves obtained experimentally on the first and second layers of the triangular island. The curves were measured at a set point of $U=1$ V and $I=1$ nA. The inset shows a topography image of the sample prepared at 550 K and indicates the area where spectroscopy measurements were performed. The scan size is 240×170 nm^2.

therefore hcp islands. These findings show that the electronic structures are nonequivalent for the two types of islands.

On the top of the triangular Co islands, the second layer can be formed. The dI/dU spectrum of the second-layer islands is shown in Fig. 3. The pronounced peak at +0.2 eV, which is a fingerprint for Co islands at 300 K is absent. This suggests that the second layer of the islands grown at high temperature is possibly an alloy or a capping layer of Pd. Christensen *et al.*[12] calculated segregation energies and surface mixing energies for all combinations of the transition and noble metals for closed packed surfaces. For Co and Pd(111) a segregation energy of +0.40 eV/atom was found; i.e., deposited Co atoms do not stay on the surface but tend to be covered by Pd. Further, a mixing energy of +0.40 eV/atom was found, leading to alloying.

V. ELECTRONIC STRUCTURE OF ISLANDS GROWN AT 300 K

In the next step we focus on the electronic structure of double-layer islands. To investigate the electronic structure of these islands grown at 300 K in detail, spatially resolved dI/dU spectra were measured for 0.4 ML Co. In order to gather information about the double-layer (DL) islands, STS measurements have been performed at various locations on the island [see Fig. 4(a)]. STS spectra were recorded on the Pd substrate, at the edge, the center of the island, and the bright crossing points of the dislocation lines. In Figs. 4(a) and 5(a), there are two kinds of spots visible at the crossing points: white and gray spots. They are also depicted in the line scan in Fig. 4(c). The gray spots (height of ~1 Å) are correlated with the crossing point of dislocation lines and they are labeled "on-top." The white spots (height of ~2 Å), represent "clusters" which contain additional atoms in the third layer decorating the crossing points, as will be shown below. For all marked points in the topography, spectra are drawn in Figs. 4(d) and 4(e). Note that the spectra in Fig. 4(d) for the center of the island are averaged curves for the inner island without the edge. The dislocation pattern which is observed on the top of the islands and its electronic features will be described in Sec. V A.

The spectroscopic data reveal that the major peaks for the DL island are observed near the Fermi level at $U=-0.45$ eV and at +0.2 eV. The tunneling spectrum for the clean Pd(111) substrate is shown for comparison. It differs from the Co spectrum. Therefore, chemical-selective imaging can be performed by selecting an appropriate sample bias voltage U. The dI/dU curve for Pd(111) shows several peaks: a pronounced filled-state peak (a negative sample bias corresponds to filled states and a positive one to empty states) at about $U=-0.4$ eV as well as a peak at about −0.1 eV. These observations are similar to earlier low-temperature tunneling spectroscopy results for Pd single crystals.[13] The peak at −0.4 eV corresponds to a surface resonance.[14] Note that in STS data for Pd(111), this peak was not always observed; i.e., it could also be a contribution from a tip.

Figures 4(b) and 4(d) show the results of STS measurements on the edge of the island. The surface state at +0.2 eV on the islands shifts up to +0.25 eV at the edge. Possibly the shift of the surface state is related to a partial relaxation of Co. As the Co atoms may shift inward, thus bringing the lattice spacing closer to the Co bulk value, the surface-state energy shifts up. A similar stress-induced change in electronic structure in Fe/W(110) was observed by Bode *et al.*[15,16] Additionally, we observed a broadened peak between −0.45 and −0.15 V. This broad feature can be an indication of Co/Pd intermixing at the island edge, or it might be related to the relaxation of Co atoms at the edge of the island. The dI/dU spectrum for the cluster [cf. Fig. 4(e)] exhibits a weak shoulder at +0.34 eV and a peak at −0.5 eV. This information was obtained by fitting Lorentzians to the data. A closer analysis of the data shows that these clusters are the beginning of the third monolayer because the third monolayer likely starts to nucleate at the crossing point of the dislocation lines [cf. Fig. 4(c)]. This was deduced from STS measurements of the third layer on the top of DL island. The spectroscopic data of the third ML reveal a shoulder at +0.34 eV, which corresponds to the surface state at +0.2 eV for a cluster of DL island [cf. Fig. 4(e)]. However, it is shifted due to the larger number of atoms in a cluster of the third layer.

A. Dislocation pattern of DL islands

The reconstruction of the Au(111) surface with hcp and fcc stackings was addressed by Chen *et al.*[17] and Bürgi *et al.*[18] In literature, the electronic structure of fcc and hcp Co islands on Cu(111) (Ref. 7) as well as fcc and hcp Co on W(110) (Ref. 19) were reported. It was shown by means of experiments and theoretical calculations that the spectrum for faulted structures exhibits a higher peak intensity and is shifted in the energy in comparison to a peak for fcc structures. In order to study how the dislocation pattern influences the electronic properties of Co/Pd(111), we performed tunneling spectroscopy at 77 K in the hcp and fcc regions of the

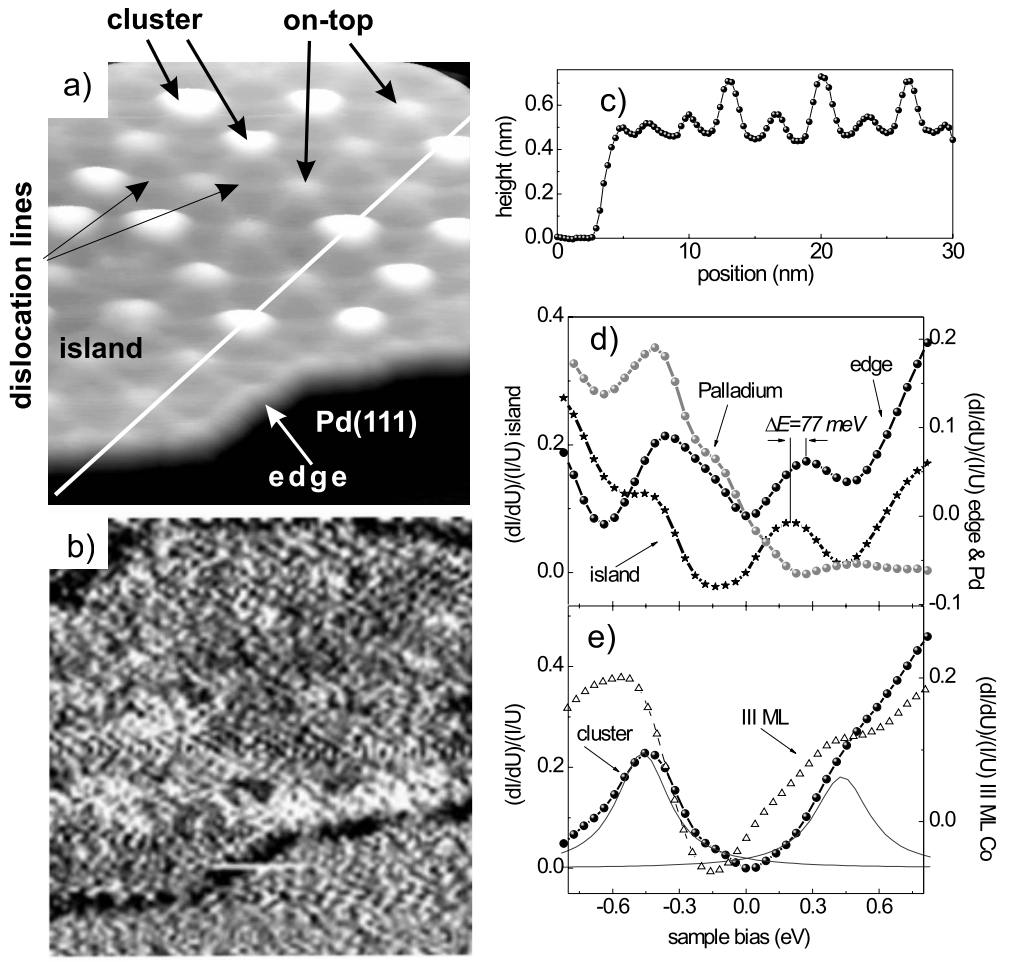

FIG. 4. (a) STM topography showing a DL island prepared at 300 K (coverage of 0.4 ML, size of 22.2×20.3 nm^2, $I=1$ nA and $U=0.5$ V). The image is displayed in a three-dimensional view. (b) dI/dU map at $U=-0.64$ V, showing clearly the edge of the islands as a black line. (c) The line profile along the white line in (a). (d) Normalized dI/dU curves of the Pd(111) substrate, the island, and the edge of the island. (e) The normalized dI/dU spectrum measured on the third monolayer on the DL island at 300 K compared to the normalized dI/dU curve taken on additional Co atoms on top labeled "cluster" at 77 K. The thin solid lines are Lorentzian fits.

reconstructed unit cell. Figure 5(a) shows a constant current topography image which includes several regular hcp and fcc regions separated by dislocations lines. These lines appear slightly higher and are formed by Co atoms taking bridge positions separating fcc and hcp regions. As a substrate is of fcc symmetry (i.e., of only threefold symmetry) dislocations line appear along the $[1\bar{1}0]$ direction of the substrate [see Fig. 5(a)] and the $[\bar{1}12]$ plane, separating fcc and hcp stacking, is by crystallography not a mirror plane. From this follows that the triangular areas with corners in the $[\bar{1}12]$ direction are fcc areas.

The spectra for fcc and hcp stackings, the dislocation line between the two stackings, and the on-top position at the crossing of the dislocation lines are shown in Figs. 5(b) and 5(c). Spectra from the two regions were separately averaged before plotting. As seen in Fig. 5(c), both (fcc and hcp) regions of the pattern show nearly identical features, a peak near +0.25 eV, and a shoulder near −0.4 eV sample bias. However, the peak positions are slightly shifted. The hcp spectrum shows a peak at higher energy for positive bias and a shoulder at lower energies for negative voltages compared to the fcc spectrum. The energy shift is $\Delta E\approx125$ meV.

We also measured the dI/dU spectra for the dislocation line and the on-top position in the dislocation pattern. In the dislocation line some atoms are forced away from threefold hollow sites just between fcc and hcp structures. This result is confirmed by our STS experiments, as the spectrum recorded over the dislocation line exhibits peaks in the middle position between hcp and fcc structures, i.e., at $E=-0.39$ and +0.23 eV. However the dI/dU spectrum of the on-top position shows a surface state shifted to +0.11 eV and a small shoulder at $E=-0.39$ eV. We note that the spectra recorded over the fcc, hcp, on-top position, and the dislocation line all have a peak at +0.82 eV, which is independent of the stacking. The dI/dU spectra in Fig. 5 can be interpreted by noting that STS corresponds to a convolution of the tip and surface LDOS. If the same STM tip is used to measure dI/dU at different points on a surface, then differences in dI/dU must arise from differences in the surface LDOS. This allows to interpret the differences in the spectra in Figs. 5(b) and 5(c) as representative of the difference in electronic LDOS between hcp and fcc regions of the dislocation network. An additional difference between fcc and hcp stackings is best

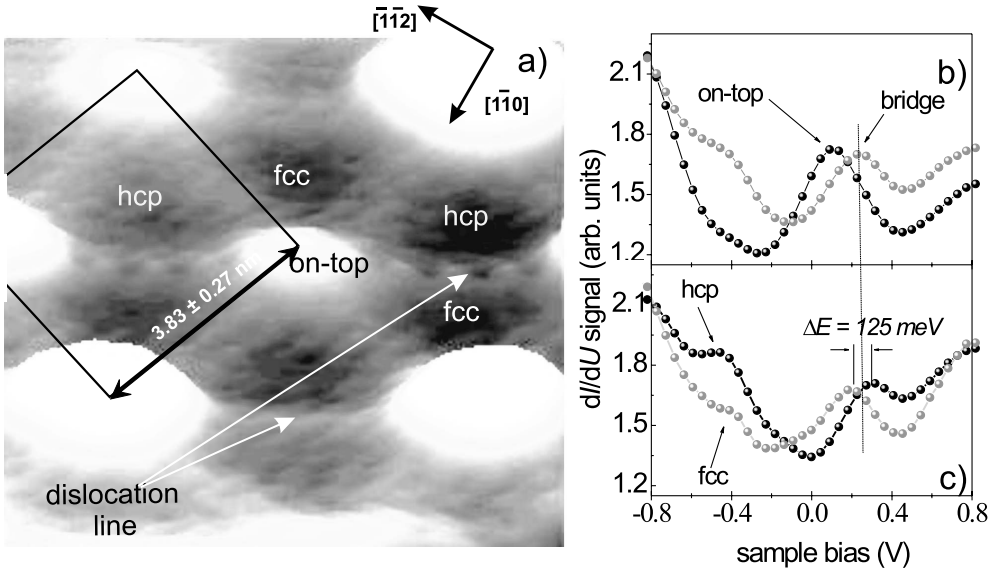

FIG. 5. (a) STM image of the dislocation network displayed in a three-dimensional view (size: 5.8×8.1 nm^2). Tunneling parameters: $U=-0.547$ V and $I=0.5$ nA. Also shown is the spatially averaged dI/dU curve of the dislocation structure of Co DL island at a set point $U=0.5$ V and $I=1$ nA. (c) dI/dU curves taken on the dislocation line and at on-top position. (d) dI/dU curves obtained on the fcc and hcp stackings. The line marks the position of peak for the dislocation line.

seen in Fig. 5(c), where the peak at 0.48 eV below E_F is much more pronounced in the hcp region as compared to the fcc region.

Despite the fact that the DOS of the tip is unknown and thus imposes an unknown contribution to the structure observed in dI/dU spectra, the following features have been observed in all spectra: the difference in STS spectra recorded for the hcp and fcc regions of the dislocation pattern, i.e., shifted position of surface state in the spectra, is in accord with previous findings for Co/Cu(111) (Refs. 6, 7, and 20) and Co/W(110) (Ref. 19) and was observed in Co islands prepared at 550 K.

B. Out-of-plane spin contrast of DL islands

Previous experiments showed that the magnetic easy axis for film thickness below 1 ML points along the surface normal.[21] Therefore, we used Cr coated W tips,[22] which exhibit an out-of-plane spin polarization, to study the magnetic structure of the Co islands with spin-polarized scanning tunneling spectroscopy. In SP-STS, the local differential conductance dI/dU depends on the relative direction of tip and sample spin polarization. Figure 6(a) shows the topography obtained with a Cr coated W tip on 0.4 ML Co/Pd(111), while Fig. 6(b) shows the dI/dU map of the same area at +0.2 eV. This map reveals a strong dark-bright contrast between islands A and B. Full spectroscopy curves taken above both islands are displayed in Fig. 6(c). The dI/dU curves obtained with the 25 ML Cr coated tip show clear differences. While the peak positions in both spectra are identical, the peak heights vary. This indicates identical electronic structures but different spin polarizations; i.e., the contrast is caused by a spin-polarized surface state. White (gray) islands are magnetized parallel (antiparallel) to the tip magnetization. A schematic drawing of the Co islands on the Pd(111) and Cr coated W tip is shown in Fig. 6(d). Arrows denote the magnetization directions of the islands and of the tip's last atom, which carries the tunneling current.

Such a contrast was observed only with Cr coated W tips. It was never observed with bare W tips. Additionally, a reverse contrast was observed using the same Cr coated tip but at a later time. During the time between the images, the apex atom of the tip most likely changed such that the tip spin-polarization was reversed. This change demonstrated the degree of freedom of the tip polarization direction. Figure 6(e) shows a topographic image with larger scale of the same area of sample as in Fig. 6(a). Figure 6(f) is the dI/dU map at +0.20 eV, which was measured at the same set point, 1 h later. Figure 6(f) shows a clear contrast, but the contrast is reversed compared to that in Fig. 6(b). We exclude a change in the sample magnetization because the magneto-optic Kerr effect (MOKE) measurements show that films below 1 ML are out-of-plane magnetized with high coercivity.[21] We propose that the surface state at +0.2 eV in DL islands has majority character, in agreement with the surface state of bulk Co(0001).[23]

VI. DISCUSSION

We observed a peak around +0.2 eV for all Co DL islands prepared below 340 K. This spectral feature is likely the expected surface state, which was predicted in calculations by Barral *et al.*[24] and observed by Ding *et al.*[23] for bulk Co(0001). In spin- and layer-resolved spectral density of Co(0001) bulk for the first four surface layers, they observed the surface state at $U=+0.2$ eV and $U=-0.5$ eV. The experimentally determined position of the surface state in Co DL islands is similar to the theoretical prediction. Also, there is general agreement between theoretical density of states of Co(0001) and the experimental differential conductance in

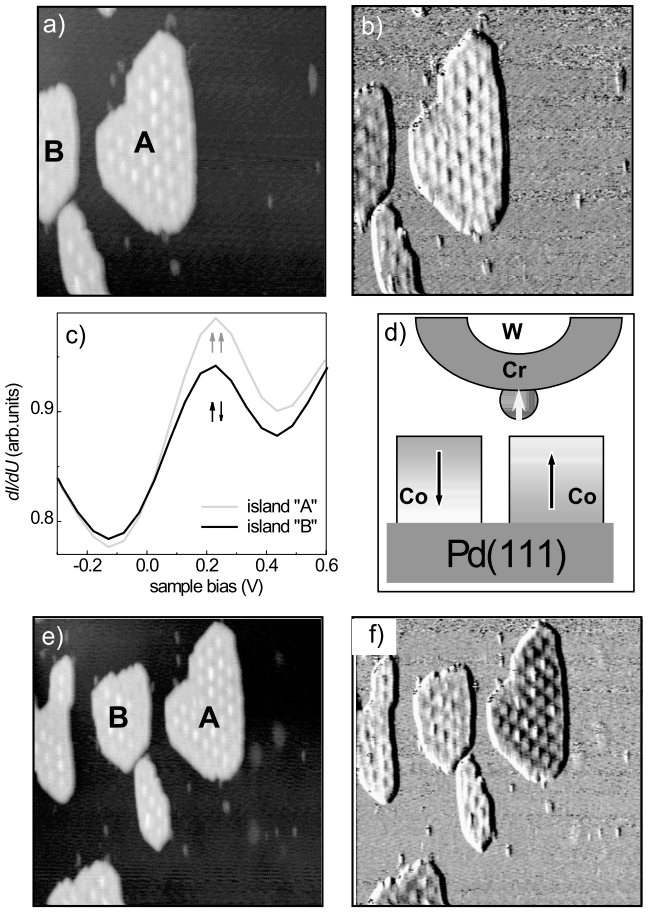

FIG. 6. SP-STS measurements of 0.4 ML Co on Pd(111) grown at 300 K showing magnetic contrast at $T=77$ K. These measurements were performed with a Cr coated W tip. (a) Topographic image and (b) dI/dU map obtained at $U=+0.2$ eV and $I=0.5$ nA (50×50 nm^2). The labels A and B denote the areas for which SP-STS curves were obtained. (c) shows the corresponding dI/dU curves, which were obtained at a set point $I=1$ nA and $U=1$ V. (d) reveals a model of the magnetization directions between the tip's last atom and the sample. (e) topographic image and (f) dI/dU map obtained at $U=+0.2$ eV and $I=0.5$ nA (62×62 nm^2). The labels A and B denote the same areas as in (a) and (f). Here the dI/dU map (f) shows a reversed magnetic contrast.

the whole energy region shown. This is an indication that at room temperature Co grows on Pd(111) without strong Co/Pd intermixing. However, quantitative agreement with the experimental data is rather surprising because Co monolayers and double layers interact strongly with the Pd(111) substrate, whereas the theoretical calculations are for bulk Co. Spin-resolved inverse photoemission spectroscopy (SR-IPS) on a 20-ML-thick hcp Co film grown on a W(110) substrate have shown peaks located just above the Fermi energy at +0.25 and +0.75 eV.[25] This experimental result gives us an additional proof of the existence of a surface state at +0.2 eV for Co. We note that we also observe a peak at +0.75 eV but only for Co films prepared at 300 and at 550 K above 5 ML coverage. We propose that this peak for the thicker regime is related to bulk states of cobalt.

The peak at -0.40 ± 0.08 eV, which shifted depending on stacking and size of islands, was detected for the double-layer islands. The nature of the occupied surface state observed in photoemission at −0.3 eV (Ref. 26) is still not clear. At this energy, the electronic structure of the Co surface on Cu(111) and W(110) is very sensitive to stacking.[7,19,20,27] Early angle-resolved ultraviolet photoemission spectroscopy (ARUPS) measurements claimed an *sp*-like surface state at −0.3 eV,[26,28] later ascribed to a $d_{3z^2-r^2}$-like state.[29] Some STS experiments confirm this state by showing a peak at −0.31 eV or at a slightly lower energy of −0.43 eV. The last value is confirmed by our STS measurements with clean W tips. Finally, the state at −0.3 eV was assigned to the surface resonance by Wiebe *et al.*[19]

Two groups experimentally studied the electronic properties of Co layers on Pd(111) prepared at 300 K. Sawada *et al.*[30] and Kang *et al.*[31] investigated the thickness dependence of the valence band structure of Co/Pd(111) with spin-resolved photoelectron spectroscopy (SARPES). They found that the hybridization between the Co 3*d* and the Pd 4*d* states causes a binding-energy shift of Pd states. They showed that the appearance of perpendicular magnetic anisotropy in the monolayer regime and the reorientation of the magnetization direction are explained by the thickness dependence of the Co 3*d* states. In our experiment, we performed measurements for submonolayer regime. For this reason, it is hard to compare electronic structures obtained by means of SARPES and STS. In our STS measurements, we have observed that the dI/dU curves change with thickness; i.e., the surface state shifted with thickness. An advantage of STS measurements is, however, the ability to get information about local thickness in comparison to ARUPS or SR-IPS. To correlate electronic structure with magnetic properties, we performed spin-polarized spectroscopy for islands grown at 300 K. The electronic state at +0.2 eV is a spin-polarized surface state of majority character.[23]

Two distinct island orientations were found for the epitaxial Co growth on Pd(111). The electronic structure of fcc and hcp islands has been studied experimentally by several groups with STM and a theoretical analysis of these observations was also performed. Wiebe *et al.*[19] and Pietzsch *et al.*[7] claimed that the peak at −0.3 eV is sensitive to the stacking at the continuous film or island surface as well as to dislocation lines. In contrast, Vazquez de Parga *et al.*[6] found no spectroscopic difference below E_F. In our experiment the surface state at above and below E_F depends on stacking, which lead to the conclusion that the energy of the cobalt surface state is correlated with the nature of the hollow site (fcc and hcp) of Pd(111).

The surface state is also manifested in the apparent island heights as a function of the bias voltage. Below the surface-state energy, the islands have a height close to the geometric heights. At energies of the surface state peak, however, the islands appear significantly higher. This is related to the extension of the surface state of Co into the vacuum. It is also sensitive to the exact surface-state energy, as deduced from the different apparent heights of fcc and hcp islands. Although we qualitatively understood this effect, the magnitude of the effect is surprising and needs a more detailed study as *ab initio* calculation.

VII. SUMMARY AND OUTLOOK

In summary, we have investigated the shape and electronic structure of Co islands grown on Pd(111) by means of scanning tunneling microscopy. The shape of Co islands on Pd(111) is strongly temperature dependent. The islands can exhibit three principally different shapes. The first one is observed at 180 K and consists of fairly irregular islands due to a limited edge diffusion. The second one we observed is hexagonal islands at 300 K with a hexagonal dislocation pattern. Finally, at high temperatures, the islands are characterized by an overall triangular shape. The orientation of the islands is related to their stacking.

The presented STM and STS measurements lead to understanding of the electronic properties of Cobalt on Pd(111) in the submonolayer regime. The electronic structure of the island prepared at different temperatures is different. In the monolayer regime for samples prepared at 300 and 550 K, the peaks in dI/dU are at similar energies but the shapes of the dI/dU curves are different. We found peaks at +0.2 eV and below this energy for all islands prepared at the two selected temperatures. This spectral feature is likely the expected surface state. To investigate the ferromagnetic nature of the Co films and to correlate their electronic structure and magnetic properties, spin-polarized STS experiments were carried out. We showed that Co islands with dislocation network prepared at 300 K display an out-of-plane spin contrast. The identification of fcc and hcp types was carried out by STS. Also, it was shown that electronic effects may have a strong influence on the apparent island height measured in STM for triangular islands.

*Corresponding author. Present address: Max-Planck-Institut für Festkörperforschung, Heisenbergstr. 1, D-70569 Stuttgart, Germany; m.wasniowska@fkf.mpg.de

[1] M. Wutting and X. Liu, *Ultrathin Metal Films* (Springer, New York, 2004).
[2] M. Michely and J. Krug, *Islands, Mounds and Atoms* (Springer, New York, 2004).
[3] R. Q. Hwang, J. Schröder, C. Günther, and R. J. Behm, Phys. Rev. Lett. **67**, 3279 (1991).
[4] K. Meinel, M. Klaua, and H. Bethge, Phys. Status Solidi A **110**, 189 (1988).
[5] C. Busse, C. Polop, M. Müller, K. Albe, U. Linke, and T. Michely, Phys. Rev. Lett. **91**, 056103 (2003).
[6] A. L. Vázquez de Parga, F. J. García-Vidal, and R. Miranda, Phys. Rev. Lett. **85**, 4365 (2000).
[7] O. Pietzsch, A. Kubetzka, M. Bode, and R. Wiesendanger, Phys. Rev. Lett. **92**, 057202 (2004).
[8] M. Wasniowska, N. Janke-Gilman, W. Wulfhekel, M. Przybylski, and J. Kirschner, Surf. Sci. **601**, 3073 (2007).
[9] W. Wulfhekel, F. Zavaliche, R. Hertel, S. Bodea, G. Steierl, G. Liu, J. Kirschner, and H. P. Oepen, Phys. Rev. B **68**, 144416 (2003).
[10] R. Schwoebel and E. Shipsey, J. Appl. Phys. **37**, 3682 (1966).
[11] M. V. Rastei, J. P. Bucher, P. A. Ignatiev, V. S. Stepanyuk, and P. Bruno, Phys. Rev. B **75**, 045436 (2007).
[12] A. Christensen, A. V. Ruban, P. Stoltze, K. W. Jacobsen, H. L. Skriver, J. K. Nørskov, and F. Besenbacher, Phys. Rev. B **56**, 5822 (1997).
[13] S. Speller, T. Rauch, A. Postnikov, and W. Heiland, Phys. Rev. B **61**, 7297 (2000).
[14] D. Drakova and G. Doyen, Surf. Sci. **352-354**, 698 (1996).
[15] M. Bode, R. Pascal, M. Dreyer, and R. Wiesendanger, Phys. Rev. B **54**, R8385 (1996).
[16] M. Bode, R. Pascal, and R. Wiesendanger, Appl. Phys. A: Mater. Sci. Process. **62**, 571 (1996).
[17] W. Chen, V. Madhavan, T. Jamneala, and M. F. Crommie, Phys. Rev. Lett. **80**, 1469 (1998).
[18] L. Bürgi, H. Brune, and K. Kern, Phys. Rev. Lett. **89**, 176801 (2002).
[19] J. Wiebe, L. Sacharow, A. Wachowiak, G. Bihlmayer, S. Heinze, S. Blügel, M. Morgenstern, and R. Wiesendanger, Phys. Rev. B **70**, 035404 (2004).
[20] S. N. Okuno, T. Kishi, and K. Tanaka, Phys. Rev. Lett. **88**, 066803 (2002).
[21] M. Przybylski, L. Yan, J. Żukrowski, M. Nyvlt, Y. Shi, A. Winkelmann, J. Barthel, M. Waśniowska, and J. Kirschner, Phys. Rev. B **73**, 085413 (2006).
[22] A. Wachowiak, J. Wiebe, M. Bode, O. Pietzsch, M. Morgenstern, and R. Wiesendanger, Science **298**, 577 (2002).
[23] H. F. Ding, W. Wulfhekel, J. Henk, P. Bruno, and J. Kirschner, Phys. Rev. Lett. **90**, 116603 (2003).
[24] M. Barral, A. Llois, and M. Weissmann, Physica B (Amsterdam) **354**, 161 (2004).
[25] C. Math, J. Braun, and M. Donath, Surf. Sci. **482-485**, 556 (2001).
[26] E. Wetli, T. J. Kreutz, H. Schmid, T. Greber, J. Osterwalder, and M. Hochstrasser, Surf. Sci. **402-404**, 551 (1998).
[27] M. Pratzer and H. J. Elmers, Phys. Rev. B **72**, 035460 (2005).
[28] F. J. Himpsel and D. E. Eastman, Phys. Rev. B **20**, 3217 (1979).
[29] H. Knoppe and E. Bauer, Phys. Rev. B **48**, 1794 (1993).
[30] M. Sawada, K. Hayashi, and A. Kakizaki, J. Phys. Soc. Jpn. **72**, 1161 (2003).
[31] J. Kang, D. Hwang, J. Hong, J. Jeong, H. An, Y. Lee, J. Lee, and K. Kim, J. Magn. Magn. Mater. **150**, 323 (1995).